Adsorption and inhibiting properties of *Cleome Droserifolia* extract on the corrosion of AISI 1018 carbon steel in hydrochloric acid solution

M.E. Eissa

College of Science, Chemistry Department, Al Imam Mohammad Ibn Saud Islamic University (IMSIU), Riyadh 11623, Kingdom of Saudi Arabia
E-mail: miissa@imamu.edu.sa

Abstract

The inhibitory effect using *Cleome droserifolia* extract as corrosion inhibitor for 1018 carbon steel (CS) in one molar hydrochloric acid has been studied. This study was carried out using chemical methods such as mass loss method (ML), DC potentiodynamic polarization (PDP), AC impedance (EIS), and electrochemical frequency modulation (EFM**)** techniques. Results obtained from these methods showed that with increasing the concentration of *Cleome droserifolia* extract the inhibition efficiency (%*IE*) increases and reaches 92.1% at 600 ppm, 25°C from the ML method. The adsorption of these derivatives on the CS surface was used to explain the inhibition. According to the values of ΔG^0_{ads}, which ranged from 16.8 to 18.3 kJ·mol^{-1}, the adsorption of the extract molecules on the CS surface is physical adsorption. The inhibitor was of mixed kind according to the polarization curves (it affects both anodic and cathodic processes). It was found that these derivatives follow Langmuir adsorption isotherm. Several surface inspection methods have been used. Also, surface checks were utilized to illustrate the importance of this *Cleome droserifolia* extract to prevent corrosion process for CS. It was found that all of these used methods are in agreement with each other.

Received: September 22, 2023. Published: January 21, 2024 doi: 10.17675/2305-6894-2024-13-1-8

Keywords: *corrosion inhibition, carbon steel, HCl, Cleome droserifolia extract, Langmuir isotherm, PDP, EIS, EFM, AFM.*

1. Introduction

Many industries use CS, including oil and gas refineries, bridges, petroleum industries and machinery. This makes it a popular choice for modern road construction, pipe and support. Like tubes, carbon steel can be very thin compared to other metals. HCl is used to remove the oxide layer formed on CS surface, pickling of metals, cleaning of boilers, acidizing of oil wells, and recovery of ion exchangers [1]. This acid causes the corrosion process of the CS [2]. In addition to the previous, HCl is one of the acids that are widely used in improving the productivity (stimulation) of wells in oil and gas production, and over several years is utilized to raise the primary efficiency of new wells as well as restore the efficiency of old

wells [3, 4]. A corrosion inhibitor is a chemical that efficiently slows the rate of corrosion of a metal exposed to that environment when applied to it at a tiny quantity [5]. Plant extracts corrosion inhibitors are environmentally friendly, available, inexpensive, and sources for obtaining them are renewable [6–16].

As a result, utilizing ML and electrochemical techniques, the current research describes a study of the corrosion protective activity of *Cleome droserifolia* on CS corrosion in 1 M hydrochloric acid solution. The inhibition efficiency at altered concentrations of inhibitors in acidic media was investigated and discussed. Temperature effects on CS dissolving in free and inhibited acid solutions were also investigated.

2. Experimental

2.1. Materials and reagent

The composition of CS is: C 0.15–0.20%, Mn 0.6–0.9%, P<0.040%, S<0.050%, and Fe balance. Hydrochloric acid was utilized as corrosive medium and prepared by using a reagent of analytical grade HCl 37% then complete it by bi-distilled water. The concentration of the acid was checked by titration with standard solution of sodium carbonate solution. All chemical utilized were from BDH grades and used as received. The CS sheet of thickness 0.2 cm was mechanically press-cut into 2×2 cm coupons for ML tests. The coupons were abraded by different grades of emery papers, washed, degreased with acetone and dried. Proper doses of the acid were prepared utilizing bi-distilled water. *Cleome droserifolia* extract doses varied between (100–600 ppm) in 1.0 M HCl.

2.2. Plant extract preparation and chemical structures of major constituents

Plant material was gotten from the Suez-Cairo desert road, Egypt. The air-dried powdered *Cleome droserifolia* (600 g) was extracted with 70% ethanol. The residue left after distillation of the solvent (75 g) was successively fractionated using Soxhlet extraction was performed according to the standardized Soxhlet procedure, with 96% ethanol for 6 h. The obtained extracts were then filtered and evaporated under reduced pressure at 40°C until dryness. The dried extracts were stored at 4°C protected from the light until analysis. The extract of the *Cleome droserifolia* plant composed from multi natural organic compounds such as substituted thiocyanate, carotols, flavonoids and terpenoids and several phenolic compounds. These naturally occurring organic substances are rich with hetero atoms such as oxygen, nitrogen, and sulfur substituents. Some of these naturally occurring substances, such as terpenoids are large branched and diverse class of organic compounds with different molecular formulas such as $C_{15}H_{26}O_2$ (25 mg/ml), $C_{34}H_{52}O_7$ (5 mg/ml) and $C_{35}H_{58}O_6$ [17]. *Cleome droserifolia* shrub represents a novel source of secondary active metabolites that can be employed as antibiotic alternative in the livestock production field and/or in human pharmaceutical applications.

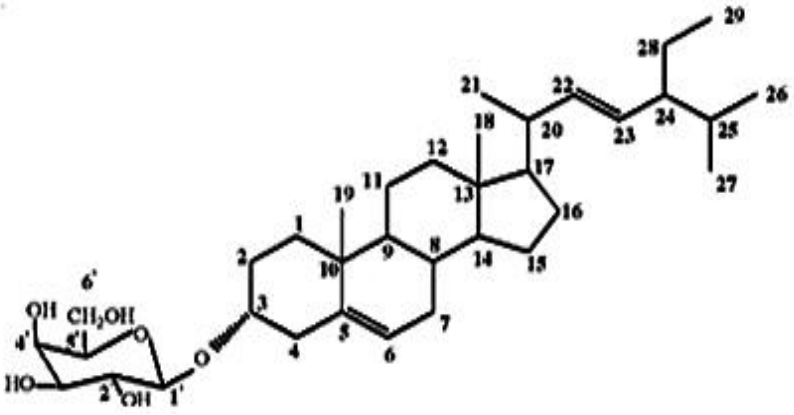

$C_{35}H_{58}O_6$

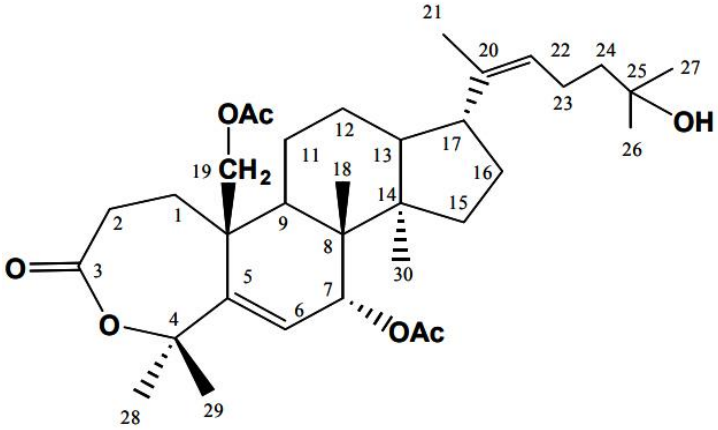

$C_{34}H_{52}O_7$

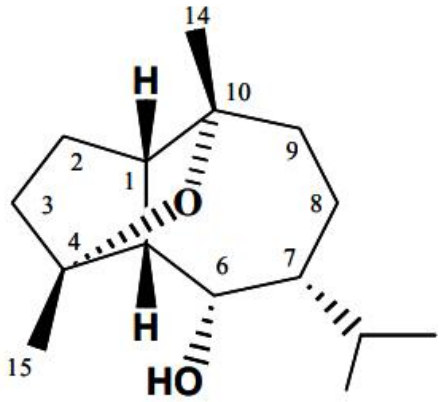

$C_{15}H_{26}O_2$

Figure 1. The main components gained from the *Cleome droserifolia* extract.

2.3. Mass Loss (ML) tests

We cut the CS metal into six pieces, each of them (20×20×2 mm). Before conducting the experiment, we sand the pieces using sand paper from coarse to fine grades from (200–2000). Then we wash the pieces using distilled water, then acetone and dry them. By the aid of glass hooks in order to the whole surface of CS samples is completely immersed and uniformly attacked by corrosive solution [18, 19]. The first piece is placed in 1 M HCl. The other pieces are putted in acid concentration with various concentrations of *Cleome droserifolia* extract (100 ppm to 600 ppm). After sanding and drying the pieces are weighed. The experiment takes three hours. This experiment is repeated at altered temperatures from (25 to 45°C). The following equations were used to compute the rate of corrosion (*CR*), the inhibition efficiency (%*IE*), and the surface coverage (θ):

$$\%IE = [1-(\Delta W_{\text{inh}} / \Delta W_{\text{free}})]\times 100 = \theta \times 100 \quad (1)$$

$$CR = \Delta W / A \cdot t \quad (2)$$

ΔW_{inh} and ΔW_{free} are the MLs in inhibitor presence and absence, respectively, the area (A) is measured in cm^{-2}, and the time (t) is measured in minutes.

2.4. Electrochemical tests

Two separate electrochemical techniques were used to test the corrosion features of CS in 100 ml of one molar HCl with and without the researched *Cleome droserifolia* extract. All of these procedures were carried out in a 25°C electrochemical glass cell with three electrode systems. As the working electrode, a 1 cm^2 CS specimen is used. Saturated calomel electrode (SCE) serves as the reference electrode, while platinum serves as the auxiliary electrode. To produce the working electrode, a CS sheet is welded to one side of the CS specimen and perfectly encased into a glass rod, leaving one side of the CS specimen exposed to the test corrosive medium. The CS specimen is mechanically abraded using emery papers and degreased with ethanol before being cleaned with bi-distilled water and then dried between filter paper before the investigations begin. Gamry Instrument (PCI4/750) with computerized outlines operated electrochemical procedures with DC105 software for PP experiments and EIS300 software for electrochemical impedance (AC) spectroscopy techniques. For fitting, graphing, and displaying the acquired data, Echem Analyst 6.03 software was used. To obtain the PDP data, the electrode potential was automatically shifted from –1000 to 0 mV *vs.* SCE at a scan rate of 0.2 mV/s. EIS was done using ac signals at open circuit potential in the frequency range of 100 kHz to 0.1 Hz with amplitudes of 10 mV peak-to-peak [20, 21]. Electrochemical frequency modulation (EFM**)** technique was performed by using signal with 10 mV amplitude with two waves of (2, 5 Hz).

2.5. Morphology of the surface

2.5.1. AFM examination

This technique gives data about surface roughness and produce 3-D and 2-D images for metal surface [22]. AFM study of surface roughness yields the level of corrosion damage (2D and 3D pictures) for CS sheets that were treated as before. The Nano Surf Easy scan 2 Flex AFM instrument was used to perform the AFM investigation in tapping mode.

2.5.2. ATR-IR analysis

The function groups of the inhibitor molecules were investigated. Cairo Univ., Egypt, used an FT-IR spectrophotometer (Model 960 Moog, ATI Mattson Infinity Series, USA) to get an infrared spectrum [23].

3. Results and Discussion

3.1. Mass loss (ML) method

Figure 2 appears the bends of ML for CS in 1 M HCl in the presence and lack of *Cleome droserifolia* extract. From this method we can calculate (*CR*, θ, *IE*%) for CS at different temperatures (25, 30, 35, 40, 45°C) [24, 25]. These parameters were recorded in Table 1. The table appears that: *IE*% increased by raising the dose of *Cleome droserifolia* extract and the *CR* increased by raising [26].

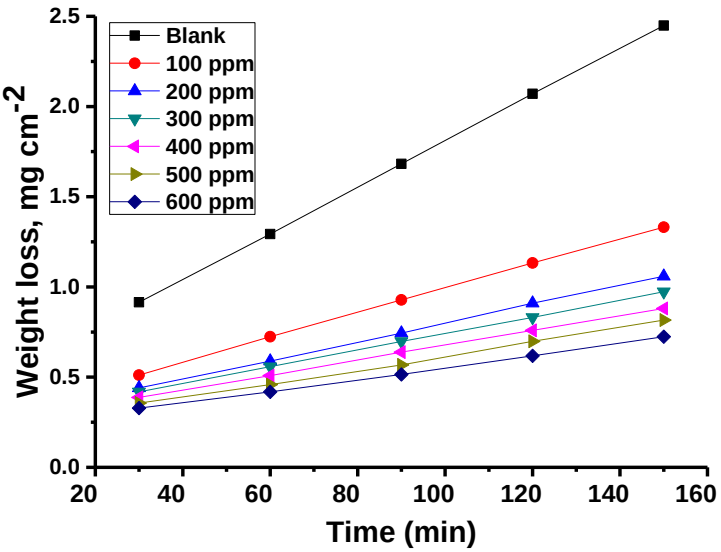

Figure 2. Time *vs.* ML diagrams of CS in 1 M HCl in the presence and absence of altered doses of *Cleome droserifolia* extract at 25°C.

Table 1. Corrosion rate values of WL measurements of CS at temperatures (25–45°C) at 120 min with and without altered doses of *Cleome droserifolia*.

[inh.] ppm	CR_{corr} (mg·cm^{-2}·h^{-1})×10^2				
	25°C	30°C	35°C	40°C	45°C
Blank	0.193	0.235	0.320	0.698	0.855
100	0.066	0.127	0.178	0.408	0.510
200	0.041	0.095	0.138	0.322	0.413
300	0.038	0.087	0.124	0.290	0.366
400	0.025	0.078	0.108	0.255	0.318
500	0.023	0.074	0.103	0.234	0.295
600	0.015	0.061	0.087	0.201	0.268

3.2. Impact of temperature

The results obtained from Table 2 showed that the *IE*% is begin to decrease with raising the temperature from 25°C to 45°C. This performance can be interpreted on the basis that the adsorption of *Cleome droserifolia* molecules on the surface of CS is physisorption [27]. As shown from Figure 3, the *IE*% increases by increasing the concentration of *Cleome droserifolia* extract at first and after that the increase was not sharp, and decreases by raising the temperature.

Table 2. List of IE% data at 120-minute dipping at altered temperatures for CS in 1.0M HCl with and absence of altered doses of *Cleome droserifolia* extract.

[inh.] ppm	IE%				
	25°C	30°C	35°C	40°C	45°C
100	66.1	46.1	44.2	41.5	40.3
200	78.6	59.2	56.8	53.9	51.7
300	80.8	63.1	61.1	58.5	57.2
400	85.1	66.7	65.9	63.5	62.8
500	88.1	68.7	67.7	66.5	65.5
600	92.1	73.9	72.9	71.3	68.7

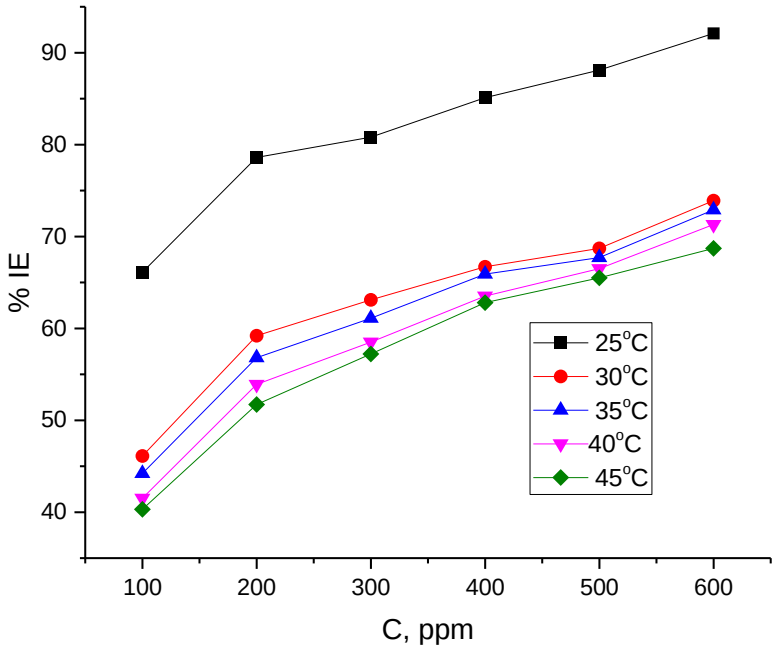

Figure 3. *%IE vs. T* (temperature) for altered doses of *Cleome droserifolia* extract.

3.3. Activation parameters

Activation results have used to illustrate the mechanism of the reaction between *Cleome droserifolia* extract and CS surface. Arrhenius equations have utilized to explain this mechanism as in (Equations 3, 4).

$$k_{corr} = A \cdot e^{-E_a^*/RT} \quad (3)$$

$$k_{corr} = RT / Nh \cdot e^{(\Delta S^*/R)} e^{(-\Delta H^*/RT)} \quad (4)$$

where E_a^*, $\Delta H^*$and $\Delta S^*$are activation energy, enthalpy and the entropy, respectively. The outcome parameters can be detected by drawing logk_{corr} *vs.* 1/*T* (Figure 4) which gives a straight line [29]. The E_a^* determine from the slope. In order to indicate the value of other parameters we plot a linear relation between logk_{corr}/*T* and 1/*T* as in (Figure 5). From this figure we can calculate ΔH^* and ΔS^*. The activation data are recorded in (Table 3) which explained that:

1. Due to *Cleome droserifolia* extract adsorbed on CS a physical barrier formed on the surface of CS which reduced the corrosion and increase the energy barrier, so that E_a^* increase in presence of *Cleome droserifolia* extract than in lack of it.
2. The negative ΔH^* indicated the presence of an exothermic reaction.
3. The negative ΔS^* because that the activated complex at the rate determining step prefer coagulation rather than a separate on the solution [30].

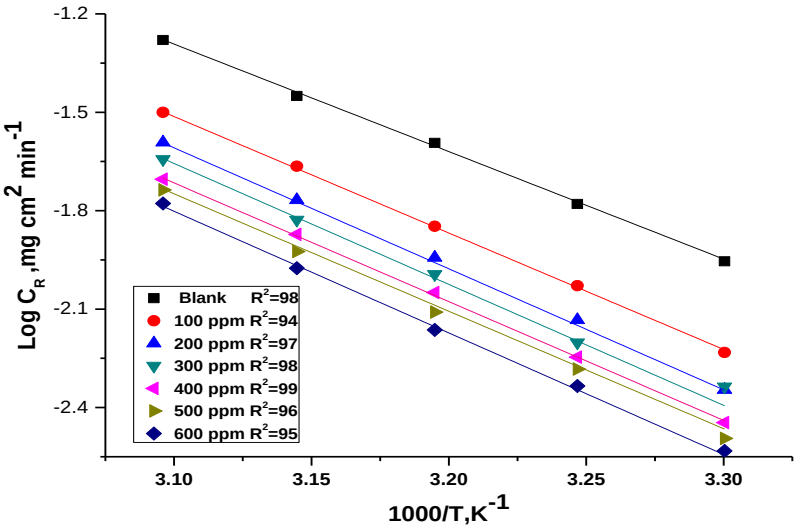

Figure 4. logk_{corr} *vs.* 1/*T* for CS in the presence and absence of *Cleome droserifolia* extract in 1 M HCl.

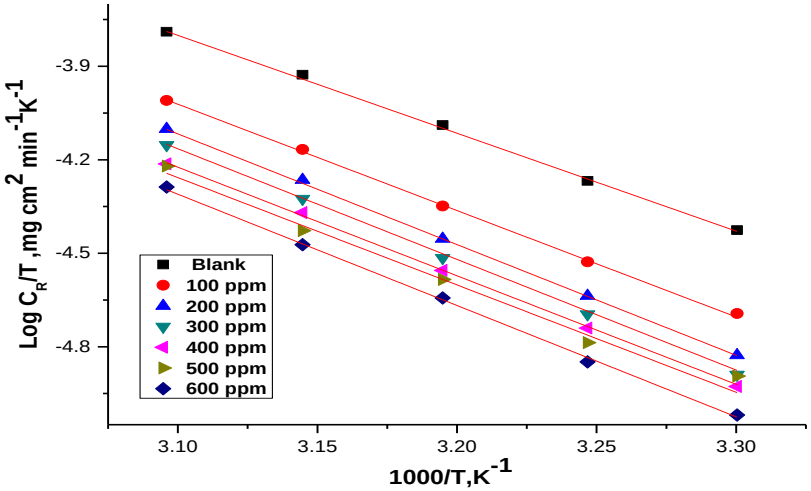

Figure 5. logk_{corr}/*T* *vs.* 1/*T* for CS in the presence and absence *Cleome droserifolia* extract in 1 M HCl.

Table 3. Activation parameters (E_a^*, ΔH^*, and ΔS^*) for CS without and with altered doses of *Cleome droserifolia* extract.

C_{inh}, ppm	E_a^*, kJ/mol	ΔH^*, kJ/mol	$-\Delta S^*$, J/mol·K
Blank	64.9	62.2	88.3
100	70.1	67.5	86.2
200	71.2	68.6	73.9
300	72.7	70.1	67.9
400	73.4	70.8	67.1

C_{inh}, ppm	E_a^*, kJ/mol	ΔH^*, kJ/mol	$-\Delta S^*$, J/mol·K
500	75.7	73.1	66.2
600	77.3	74.7	65.5

3.4. Adsorption isotherms

The behavior of adsorption of *Cleome droserifolia* extract on the surface of CS can be described by adsorption isotherm. Many adsorption processes can be utilized such as Langmuir, Temkin, Freundlich, Flory-Huggins. The excellent explanation of the adsorption process can be achieved by using Langmuir isotherm [31]. Equation 5 explain Langmuir isotherm and from it we plot the linear relation between C/θ and C which appear in in (Figure 6). ΔG^0_{ads} and K_{ads} (adsorption parameters) calculated by using Equation 6:

$$C/\theta = 1/K_{ads} + C \quad (5)$$

$$\Delta G^0_{ads} = RT\ln(K_{ads} \cdot 55.5) \quad (6)$$

where K_{ads}=constant of adsorption, and C=*Cleome droserifolia* extract concentration.

The ΔG°_{ads} data at all temperatures are known in Table 3. The (ΔH°_{ads}) was calculate approving to the Van't Hoff equation.

$$\log K_{ads} = -\Delta H^0_{ads}/2.303RT + const \quad (7)$$

Plotting ($\log K_{ads}$) *vs.* ($1/T$) give straight line as displayed in Figure 7 with the slope of ($-\Delta H^0_{ads}/2.303R$); from this slope, the ΔH^0_{ads} data was measured and is recorded in Table 4. Then by applying the next balance:

$$\Delta G^0_{ads} = \Delta H^0_{ads} - T\Delta S^0_{ads} \quad (8)$$

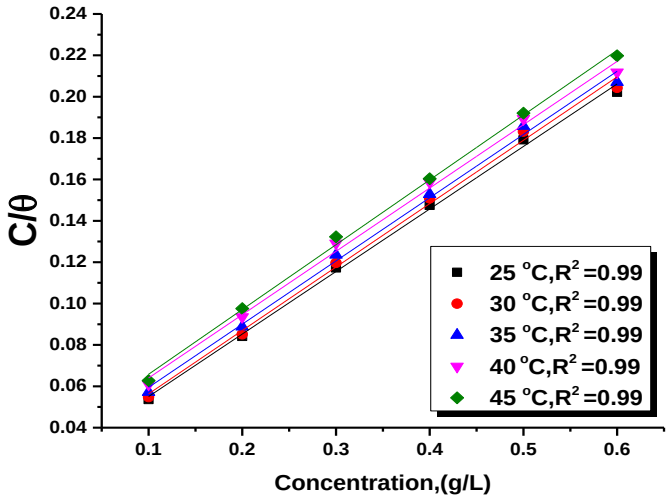

Figure 6. Curves of Langmuir adsorption on CS in the absence and presence of different doses of *Cleome droserifolia* extract.

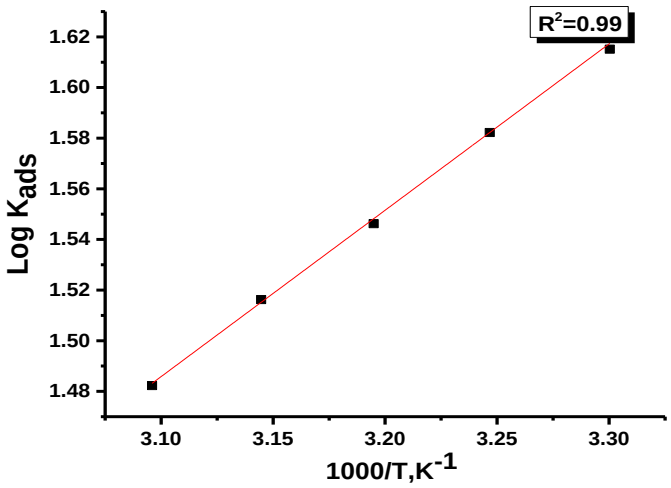

Figure 7. 1/*T vs.* logK_{ads} bends for the CS in 1.0 M HCl in the presence of *Cleome droserifolia* extract.

Table 4. Langmuir parameters of *Cleome droserifolia* extract for CS in 1.0 M HCl achieved at different temperatures.

Temp. °C	K_{ads}, M^{-1}	R^2	$-\Delta G^0_{ads}$, kJ·mol^{-1}	ΔH^0_{ads}, kJ·mol^{-1}	$-\Delta S^0_{ads}$, J·mol^{-1}·K^{-1}
298	44	0.992	18.3		64.1
303	40	0.995	17.9		62.6
308	36	0.993	17.5	29.9	61.2
313	34	0.989	17.1		59
318	30	0.992	16.8		58.3

From Table 4 we noted that [32]:

1. The adsorption parameters ΔG^0_{ads} and K_{ads} decreased when the temperature increased.
2. ΔG^0_{ads} ensure the presence of spontaneous adsorption because it's negative value.
3. The ΔG^0_{ads} data was around 20 kJ·mol^{-1} which designated the presence of physical adsorption reaction.
4. ΔH^0_{ads} have a negative sign that referred to exothermic process; this means that the adsorption process may be physical or chemical.
5. Increasing of the disorder of the motion of *Cleome droserifolia* extract in the solution gives negative ΔS^0_{ads} values.

3.5. Electrochemical tests

3.5.1. PDP tests

By plotting the logarithm current as a function of potential (Figure 8), this plot is called potentiodynamic polarization. In which an electrochemical solution's potential is formed and E_{corr} is measured, and i_{corr} from the Tafel curve (i^0_{corr}) slope is estimated, which is determined by following equation [33]:

$$\%IE = [(i_{free} - i_{inh}) / i_{free}] \times 100 \quad (9)$$

where i^0_{corr} and i_{corr} are the current in the absence and presence of *Cleome droserifoli*a extract correspondingly. From Table 5, it was found that the current density of corrosion (i_{corr}) drops as inhibitor concentration rises, indicating that the presence of *Cleome droserifolia* extract can prevent CS from dissolving, and the level of corrosion inhibition is dependent on the concentration and kind of inhibitors used. The shift in E_{corr} values did not show a clear pattern, indicating that the *Cleome droserifolia* extract studied is mixed type inhibitor [34]. The slight differences in β_a and β_c values suggest that extract impact both metal dissolution and hydrogen evolution, and the parallel Tafel lines indicate that the mechanism of the process remains unchanged.

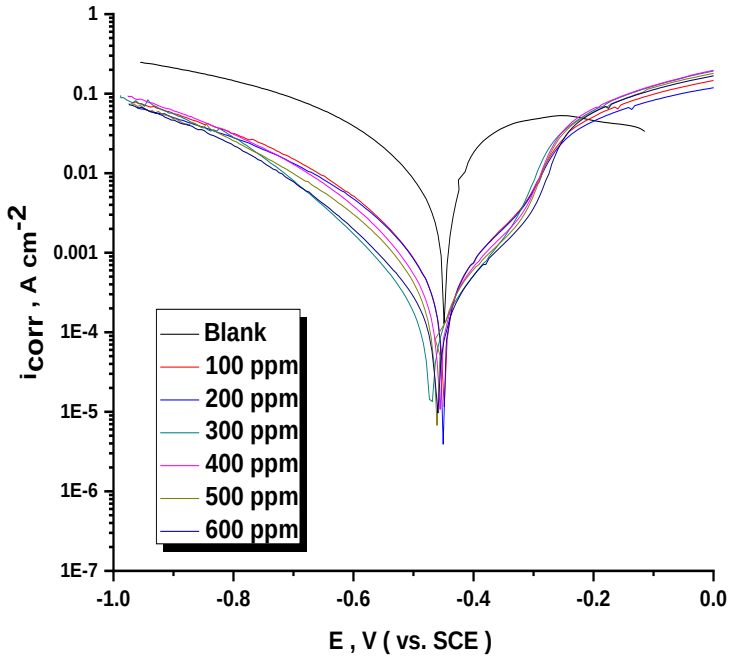

Figure 8. PDP plots of CS without and with altered doses of *Cleome droserifolia* extract at 25°C.

Table 5. Effect of *Cleome droserifolia* extract on corrosion of CS in 1.0 M HCl at 25°C.

Conc. (ppm)	$-E_{corr}$, mV *vs.* SCE	I_{corr}, mA·cm^{-2}	$-\beta_c$, mV·dec^{-1}	β_a, mV·dec^{-1}	*CR*, mpy	θ	η%
Blank	450	5210	158	125	86.4	–	–
100	476	1282	153	118	15.9	0.754	75.4
200	460	1089	146	114	13.6	0.791	79.1
300	475	917	146	121	9.4	0.824	82.4
400	466	693	144	105	8.6	0.867	86.7
500	471	604	140	108	8.1	0.884	88.4
600	458	516	147	120	6.8	0.901	90.1

3.5.2. EIS results

It showed Nyquist and Bode plots for dissolution of CS in one molar HCl in the presence and absence of *Cleome droserifolia* extract at 25°C as signified in Figure 9. The EIS diagram exhibits a nearly single semi-circuit, demonstrating that the metallic dissolution phase is accompanied by a single charge transfer mechanism that is unaffected by the presence of examined extract. The %*IE* and (θ) of the *Cleome droserifolia* extract gotten from EIS measurements using the following relationship:

$$\%IE = [(R_{ct} - R_{ct}^0) / R_{ct}] \times 100 \quad (10)$$

R_{ct} and R_{ct}^0 are the resistances existence and absence *Cleome droserifolia* extract, respectively.

Figure 10 depicts the matching circuit that defines for CS alloy and electrolyte. The diameter of Nyquist diagrams increases as the concentration of *Cleome droserifolia* extract increases due to the formation of an inhibitor-adsorbed layer on the CS surface. From Table 6, we conclude that, due to the rise in the thickness of the generated adsorbed layer, R_{ct} increases as the concentration of the examined extract improvement. C_{dl} values decrease with increasing the dose of the extract and this due to the replacement of water molecules in the double layer by adsorbed inhibitor molecules to form adherent film on CS surface, recommends that the *Cleome droserifolia* extract molecules function by adsorption at the CS/interface [35]. It is clear from Figure 9 that experimental and theoritical curves are fitting well. The small chi-squared values of χ^2 (Table 6) support good quality and equivalent circuit used. The *CPE* is inserted to substitute a double layer capacitance(C_{dl}) to provide a more precise fit and its values decreased by increasing concentration. The values of Y_0 for HCl is larger than that of inhibited electrolyte; this proposes that the extract molecules interacted with the electrode surface, thus reducing the destruction of exposed sites of the electrode.n is a measure that reflects a deviation from ideal behavior ranged from –1 to 1.

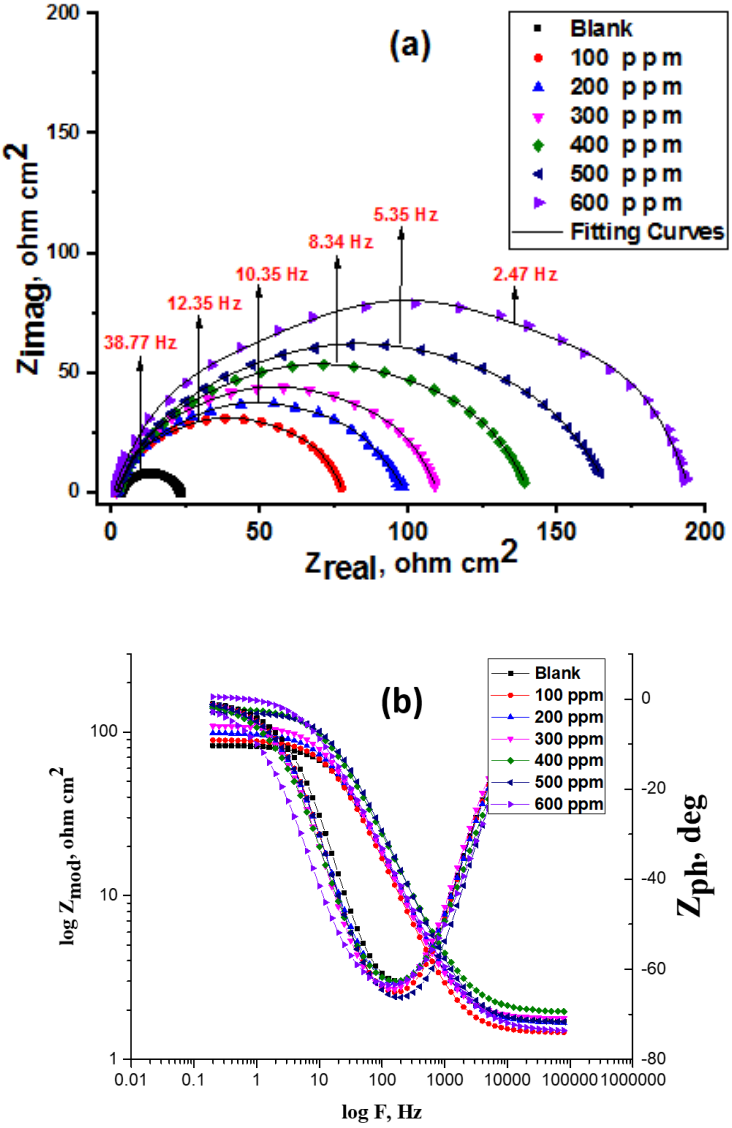

Figure 9. EIS Nyquist (a) and Bode (b) curves of CS in one molar HCl solutions in the presence of and without altered doses of *Cleome droserifolia* extract at 25°C.

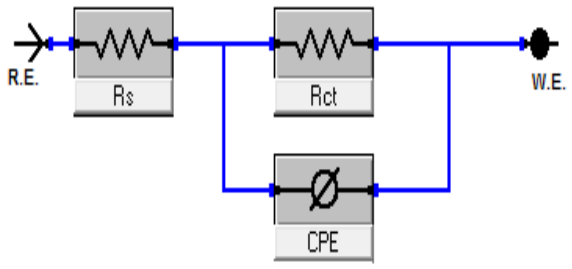

Figure 10. Circuit model utilized to match experimental EIS.

Table 6. EIS for the liquefaction of CS in one molar HCl in the presence and abcence of different doses of *Cleome droserifolia* extract at 25°C.

Conc. (ppm)	R_{ct}, Ω·cm^2	C_{dl}, μF·cm^{-2}	n	Y_0, μΩ^{-1}·s^n·cm^{-2}	θ	η%	Goodness of fit (χ^2)
Blank	25	385	0.998	389	–	–	$21.54 \cdot 10^{-3}$
100	91	135	0.985	145	0.725	72.5	$18.57 \cdot 10^{-3}$
200	111	123	0.980	133	0.775	77.5	$21.18 \cdot 10^{-3}$
300	133	112	0.975	129	0.812	81.2	$18.05 \cdot 10^{-3}$
400	139	110	0.964	125	0.820	82.0	$17.66 \cdot 10^{-3}$
500	164	107	0.949	121	0.848	84.8	$19.71 \cdot 10^{-3}$
600	200	97	0.957	116	0.875	87.5	$20.39 \cdot 10^{-3}$

3.5.3. EFM measurements

EFM utilized to detect the corrosion rate by using small signal and without using information of Tafel constant [36]. During EFM measurements a potential of two sine signals are applied to CS to produce the current. Figure 11 represents EFM curves of CS in existence and absence of altered doses of *Cleome droserifolia* extract. Corrosion parameters like (%*IE*), current density, the causality factors (CF-2 and CF-3), β_a, β_c and corrosion rate are recorded in Table 7. From the table we noted that, when the concentration of *Cleome droserifolia* extract improved the i_{corr} lowered and the %*IE* rose. The obtained data of CF-2 and CF-3 are approximate to the theoretical values (2, 3) so that the outcome results are good.

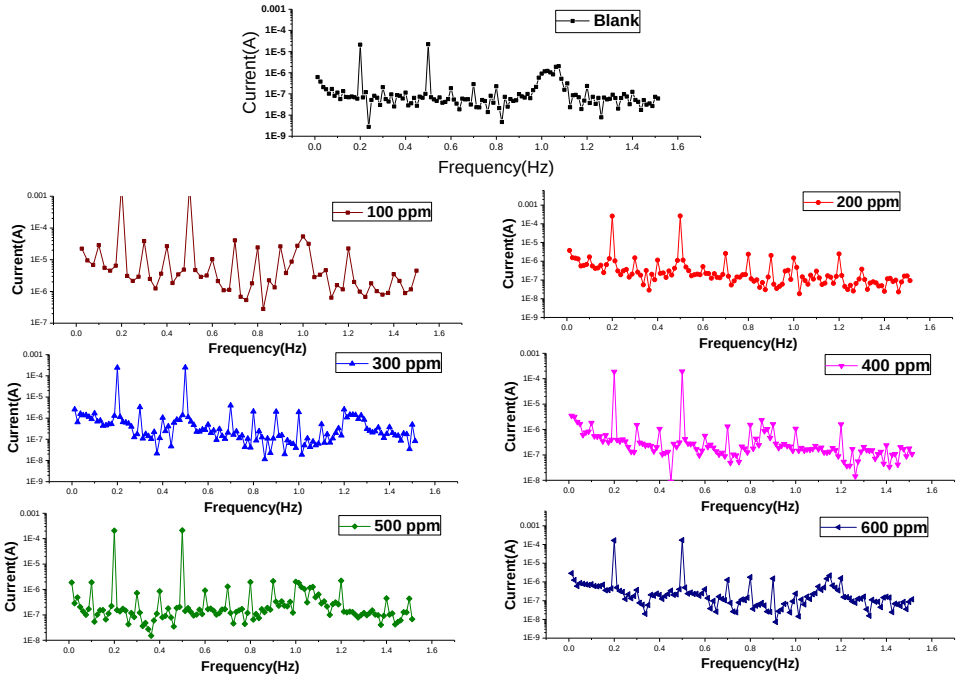

Figure 11. EFM curves of CS with and without altered doses of *Cleome droserifolia* extract.

Table 7. Outcome data of EFM for CS at various doses of *Cleome droserifolia* extract.

[inh.] ppm	i_{corr}, μA·cm^{-2}	$-\beta_c$, mV·dec^{-1}	β_a, mV·dec^{-1}	CF-2	CF-3	*CR*, mpy	θ	%*IE*
0.0	4763	120	100	2.2	3.0	118	–	–
100	1319	123	90	1.7	2.9	87	0.723	72.3
200	1115	118	80	1.9	3.0	79	0.766	76.6
300	929	115	91	2.1	3.0	73	0.805	80.5
400	867	113	93	2.2	2.9	62	0.818	81.8
500	681	116	86	1.9	3.1	58	0.857	85.7
600	457	120	90	1.9	2.8	43	0.904	90.4

3.6. Morphology of surface

3.6.1. ATR-IR examination

The FT-IR spectrophotometer is a useful tool for determining the existence of function groups in *Cleome droserifolia* extract and the type of interaction that occurs between function groups and metal surfaces [37]. Figure 12 shows broad peaks of *Cleome droserifolia* extract and *Cleome droserifolia* extract with CS. After corrosion, there are some peaks displacement between the spectra of the *Cleome droserifolia* extract and the adsorbed extract from the CS surface, and a few peaks disappear or become less noticeable. This implies that *Cleome droserifolia* extract interacts with CS through the functional groups found in *Cleome droserifolia* molecules, resulting in corrosion prevention.

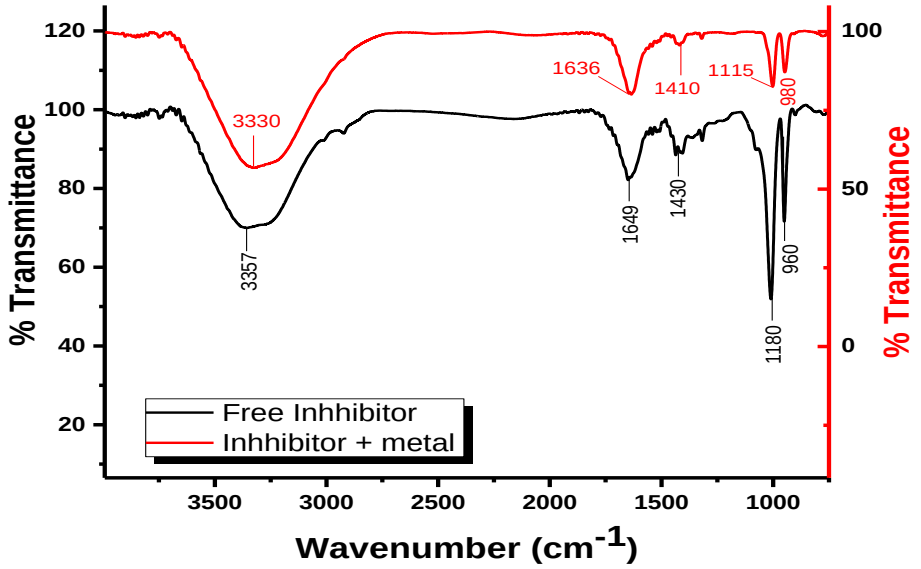

Figure 12. (a) CS ATR-FTIR after dipping in one molar HCl+300 ppm of *Cleome droserifolia* extract, (b) *Cleome droserifolia* extract before dipping.

3.6.2. AFM analysis

AFM is a great technology for observed high-resolution surface roughness analysis. AFM measurements may provide a wealth of information regarding CS surface shape, which aids in the understanding of the corrosion process. AFM roughness (Sa) for blank is 612 nm and decreased to be 211 nm for CS dipped in 1.0 M HCl and 300 ppm *Cleome droserifolia* extract From these results, it was found that, roughness of metal surface increased with immersion in one molar HCl solution due to corrosion occurs on CS surface but decreased with adding investigated extract to solution [38, 39]. This is due to the adsorption of extract molecules on CS surface.

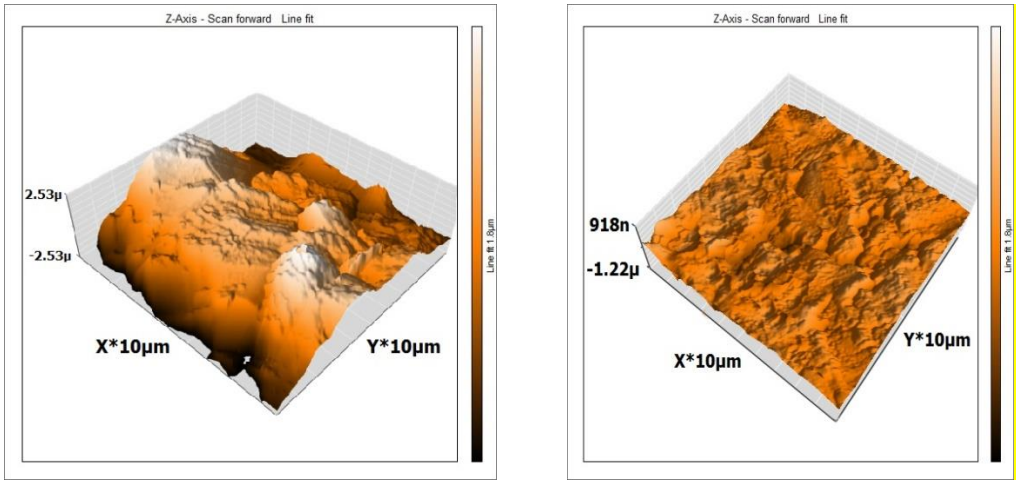

Blank With 300 ppm of C*leome droserifolia*

Figure 13. AFM images (3D) for CS surface (A) Blank (B) CS dipped in 1 M HCl enclosing 300 ppm of *Cleome droserifolia* extract.

4. Mechanism of Inhibition

From the outcome data obtained from the various tests, corrosion hindrance of CS in one molar HCl solutions by the *Cleome droserifolia* extract as designated from ML, PDP, EIS and EFM tests were depended on the nature of the inhibitor and the dose. *Cleome droserifolia* extract adsorbed layer on the CS surface, which block the active sites and decrease corrosion by preventing the attack of the surface by the corrosive medium. The Cl^- ions get adsorbed on the CS surface and turn it as negatively charged surface, the protonated inhibitors molecules (cationic) get adsorbed on the negatively charged surface of CS physically by an electrostatic attraction [40, 41]. The utilized *Cleome droserifolia* extract as corrosion protection for CS in one molar HCl had deliberated in terms of physical adsorption on the CS surface. This proved from the data of ΔG^0_{ads} (less than 20 kJ·mol^{-1}) also from the effect of temperature (%*IE* decreases by raising temperature). Figure 14 represent a schematic representation of the mechanism of the adsorption of the investigated extract molecules on the surface of CS.

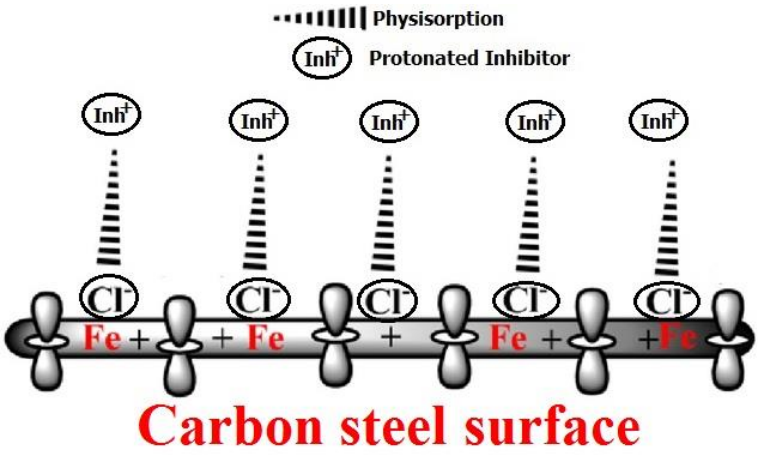

Figure 14. Mechanism of the adsorption of extract molecules on the surface of CS.

Conclusions

1. *Cleome droserifolia extract* is a fine green inhibitor which has a good inhibition effect on CS corrosion in acidic medium.
2. %*IE* increased by increasing *Cleome droserifolia* extract concentration and by lowering temperature.
3. To select the *Cleome droserifolia* extract adsorbed on the CS surface, the Langmuir isotherm was employed.
4. The polarization measurements indicated that *Cleome droserifolia* extract acts as mixed kind inhibitor.
5. Surface analysis was achieved by utilizing AFM, and FT-IR techniques.
6. EIS results indicated that by increasing the doses of *Cleome droserifolia* extract, C_{dl} decreases while R_{ct} increases, which can be attributed to adsorbed *Cleome droserifolia* molecules.
7. ML measurements are in a best agreement with electrochemical tests.

References

1. I.M. Chung, R. Malathy, S.H. Kim, K. Kalaiselvi, M. Prabakaran and M. Gopiraman, Ecofriendly green inhibitor from *Hemerocallis Fulva* against aluminum corrosion in sulphuric acid medium, *J. Adhes. Sci. Technol*., 2020, **34**, no. 14, 1483–1506. doi: 10.1080/01694243.2020.1712770
2. A.R.I. Mohammed, M.M. Solomon, K. Haruna, S.A. Umoren and T.A. Saleh, Evaluation of the corrosion inhibition efficacy of *Cola acuminata* extract for low carbon steel in simulated acid pickling environment, *Environ. Sci. Pollut. Res*., 2020, **27**, 34270–34288. doi: 10.1007/s11356-020-09636-w
3. C. Verma, M.A. Quraishi and E.E. Ebenso, Microwave and ultrasound irradiations for the synthesis of environmentally sustainable corrosion inhibitors: An overview, *Sustain. Chem. Pharm*., 2018, **10**, 134–147. doi: 10.1016/j.scp.2018.11.001

4. E.B. Agbaffa, E. Akintemi, E.A. Uduak and O.E. Oyeneyin, Corrosion inhibition potential of the methanolic crude Extract of *Mimosa pudica* leaves for mild steel in 1 m hydrochloric acid solution by weight loss method, *Sci. Lett*., 2021, **15**, no. 1, 23–42. doi: 10.24191/sl.v15i1.11791
5. V. Vorobyova and M. Skiba, Peach Pomace Extract as Efficient Sustainable Inhibitor for Carbon Steel Against Chloride-Induced Corrosion, *J. Bio- Tribo-Corros*., 2021, **7,** no. 11. DOI: 10.1007/s40735-020-00450-y
6. A. Miralrio and A.E. Vázquez, Plant Extracts as Green Corrosion Inhibitors for Different Metal Surfaces and Corrosive Media: A Review, *Processes*, 2020, **8**, no. 8, 942. doi: 10.3390/pr8080942
7. N. Bhardwaj, P. Sharma and V. Kumar, Phytochemicals as steel corrosion inhibitor: an insight into mechanism, *Corros. Rev*., 2021, **39**, 27–41. doi: 10.1515/corrrev-2020-0046
8. V. Pourzarghan and B. Fazeli-Nasab, The use of *Robinia pseudoacacia* L fruit extract as a green corrosion inhibitor in the protection of copper-based objects, *Herit. Sci*., 2021, **9**, 75. doi: 10.1186/s40494-021-00545-w
9. M. Faiz, A. Zahari, K. Awang and H. Hussin, Corrosion inhibition on mild steel in 1 M HCl solution by *Cryptocarya nigra* extracts and three of its constituents (alkaloids), *RSC Adv*., 2020, **10**, no. 11, 6547–6562. doi: 10.1039/C9RA05654H
10. M. Mohanraj and S. Aejitha, Natural *Commiphora Caudata* extract as corrosion inhibitor for mild steel in acid media, *AIP Conf. Proc*., 2020, **2270**, 050004. doi: 10.1063/5.0019569
11. R.T. Loto and C.A. Loto, Inhibition effect of *apium graveolens*, *punica granatum*, and *camellia sinensis* extracts on plain carbon steel, *Cogent Eng*., 2020, **7**, no. 1, 1798579. doi: 10.1080/23311916.2020.1798579
12. A. Zaher, A. Chaouiki, R. Salghi, A. Boukhraz, B. Bourkhiss and M. Ouhssine, Inhibition of Mild Steel Corrosion in 1 M Hydrochloric Medium by the Methanolic Extract of *Ammi visnaga* L. Lam Seeds, *Int. J. Corros*., 2020, **2020**, no. 1, 1–10. doi: 10.1155/2020/9764206
13. O.O. Ogunleye, A.O. Arinkoola, O.A. Eletta, O.O. Agbede, Y.A. Osho, A.F. Morakinyo and J.O. Hamed, Green corrosion inhibition and adsorption characteristics of *Luffa cylindrica* leaf extract on mild steel in hydrochloric acid environment, *Heliyon*, 2020, **6**, no. 1, e03205. doi: 10.1016/j.heliyon.2020.e03205
14. A.E. Ali, G.E. Badr and A.E.S. Fouda, *Citrus sinensis* Extract as a Green Inhibitor for the Corrosion of Carbon Steel in Sulphuric Acid Solution, *Biointerface Res. Appl. Chem*., 2021, **11**, no. 6, 14007–14020. doi: 10.33263/BRIAC116.1400714020
15. N.A. Reza, N.H. Akhmal, N.A. Fadil and M.F.M. Taib, A Review on Plants and Biomass Wastes as Organic Green Corrosion Inhibitors for Mild Steel in Acidic Environment, *Metals*, 2021, **11**, no. 7, 1062. doi: 10.3390/met11071062

16. S.Z. Salleh, A.H. Yusoff, S.K. Zakaria, M.A.A. Taib, A.A. Seman, M.N. Masri, M. Mohamad, S. Mamat, S.A. Sobri, A. Ali and P.T. Teo, Plant extracts as green corrosion inhibitor for ferrous metal alloys: A review, *J. Clean. Prod*., 2021, **304**, 127030. doi: 10.1016/j.jclepro.2021.127030
17. H.I. El-Askary, Terpenoid constituents from Cleome droserifolia (Forssk.) Del, *Molecules*, 2005, **10**, no. 8, 971–977. doi: 10.3390/10080971
18. A.S. Fouda, F.I. El Dossoki, A. El-Hossiany and E.A. Sello, Adsorption and Anticorrosion Behavior of Expired Meloxicam on Mild Steel in Hydrochloric Acid Solution, *Surf. Eng. Appl. Electrochem*., 2020, **56**, no. 4, 491–500. doi: 10.3103/S1068375520040055
19. P.C. Okafor, M.E. Ikpi, I.E. Uwah, E.E. Ebenso, U.J. Ekpe and S.A. Umoren, Inhibitory action of *Phyllanthus amarus* extracts on the corrosion of mild steel in acidic media, *Corros. Sci*., 2008, **50**, no. 8, 2310–2317. doi: 10.1016/j.corsci.2008.05.009
20. A.E.S. Fouda, S.M.A. Motaal, A.S. Ahmed, H.B. Sallam, A. Ezzat and A. El-Hossiany, Corrosion Protection of Carbon Steel in 2 M HCl Using *Aizoon canariense* Extract, *Biointerface Res. Appl. Chem*., 2021, **12**, no. 1, 230–243. doi: 10.33263/BRIAC121.230243
21. A.S. Fouda, S.A. Abd El-Maksoud, A. El-Hossiany and A. Ibrahim, Corrosion Protection of Stainless Steel 201 in Acidic Media Using Novel Hydrazine Derivatives as Corrosion Inhibitors, *Int. J. Electrochem. Sci*., 2019, **14**, no. 3, 2187–2207. doi: 10.20964/2019.03.15
22. A.S. Fouda, A. El-Mekabaty, I.E. Shaaban and A. El-Hossiany, Synthesis and Biological Evaluation of Novel Thiophene Derivatives as Green Inhibitors for Aluminum Corrosion in Acidic Media, *Prot. Met. Phys. Chem. Surf*., 2021, **57**, no. 5, 1060–1075. doi: 10.1134/S2070205121050075
23. O.A. Elgyar, A.M. Ouf, A. El-Hossiany and A.S. Fouda, The Inhibition Action of *Viscum Album* Extract on the Corrosion of Carbon Steel in Hydrochloric Acid Solution, *Biointerface Res. Appl. Chem*., 2021, **11**, no. 6, 14344–14358. doi: 10.33263/BRIAC116.1434414358
24. A.S. Fouda, M.A. Azeem, S.A. Mohamed, A. El-Hossiany and E. El-Desouky, Corrosion Inhibition and Adsorption Behavior of Nerium Oleander Extract on Carbon Steel in Hydrochloric Acid Solution, *Int. J. Electrochem. Sci*., 2019, **14**, no. 4, 3932–3948. doi: 10.20964/2019.04.44
25. A.S. Fouda, S. Rashwan, A. El-Hossiany and F.E. El-Morsy, Corrosion Inhibition of Zinc in Hydrochloric Acid Solution Using Some Organic Compounds as Eco-Friendly Inhibitors, *J. Chem. Biol. Phys. Sci*., 2019, **9**, no. 1, 1–24. doi: 10.24214/jcbps.A.9.1.00124
26. A.S. Fouda, S.A.A. El-Maksoud, A.A.M. Belal, A. El-Hossiany and A. Ibrahium, Effectiveness of Some Organic Compounds as Corrosion Inhibitors for Stainless Steel 201 in 1 M HCl: Experimental and Theoretical Studies, *Int. J. Electrochem. Sci*., 2018, **13**, no. 10, 9826–9846. doi: 10.20964/2018.10.36

27. A.S. Fouda, R.E. Ahmed and A. El-Hossiany, Chemical, Electrochemical and Quantum Chemical Studies for Famotidine Drug as a Safe Corrosion Inhibitor for α-Brass in HCl Solution, *Prot. Met. Phys. Chem. Surfaces*, 2021, **57**, no. 2, 398–411. doi: 10.1134/S207020512101010X
28. M. Wasim, S. Shoaib, N.M. Mubarak, Inamuddin and A.M. Asiri, Factors Influencing Corrosion of Metal Pipes in Soils, *Environ. Chem. Lett*., 2018, **16**, 861–879. doi: 10.1007/s10311-018-0731-x
29. A.S. Fouda, E.S. El-Gharkawy, H. Ramadan and A. El-Hossiany, Corrosion Resistance of Mild Steel in Hydrochloric Acid Solutions by *Clinopodium acinos* as a Green Inhibitor, *Biointerface Res. Appl. Chem*., 2021, **11**, no. 2, 9786–9803. doi: 10.33263/BRIAC112.97869803
30. A.S. Fouda, S.A.A. El-Maksoud, A. El-Hossiany and A. Ibrahim, Evolution of the Corrosion-inhibiting Efficiency of Novel Hydrazine Derivatives against Corrosion of Stainless Steel 201 in Acidic Medium, *Int. J. Electrochem. Sci*., 2019, **14**, no. 7, 6045–6064. doi: 10.20964/2019.07.65
31. A.S. Fouda, E. Abdel-Latif, H.M. Helal and A. El-Hossiany, Synthesis and Characterization of Some Novel Thiazole Derivatives and Their Applications as Corrosion Inhibitors for Zinc in 1 M Hydrochloric Acid Solution, *Russ. J. Electrochem*., 2021, **57**, 159–171. doi: 10.1134/S1023193521020105
32. A.S. Fouda, M. Eissa and A. El-Hossiany, Ciprofloxacin as Eco-Friendly Corrosion Inhibitor for Carbon Steel in Hydrochloric Acid Solution, *Int. J. Electrochem. Sci*., 2018, **13**, no. 11, 11096–11112. doi: 10.20964/2018.11.86
33. E. Fouda, A. El-Hossiany and H. Ramadan, Calotropis Procera plant extract as green corrosion inhibitor for 304 stainless steel in hydrochloric acid solution, *Zast. Mater*., 2017, **58**, 541–555. doi: 10.5937/ZASMAT1704541F
34. R. Hsissou, S. Abbout, A. Berisha, M. Berradi, M. Assouag, N. Hajjaji and A. Elharfi, Experimental, DFT and molecular dynamics simulation on the inhibition performance of the DGDCBA epoxy polymer against the corrosion of the E24 carbon steel in 1.0 M HCl solution, *J. Mol. Struct*., 2019, **1182**, 340–351. doi: 10.1016/j.molstruc.2018.12.030
35. M.A. Khaled, M.A. Ismail, A.A. El-Hossiany and A.S. Fouda, Novel pyrimidine-bichalcophene derivatives as corrosion inhibitors for copper in 1 M nitric acid solution, *RSC Adv*., 2021, **11**, no. 41, 25314–25333. doi: 10.1039/D1RA03603C
36. M.M. Motawea, A. El-Hossiany and A.S. Fouda, Corrosion Control of Copper in Nitric Acid Solution using Chenopodium Extract, *Int. J. Electrochem. Sci*., 2019, **14**, no. 2, 1372–1387. doi: 10.20964/2019.02.29
37. A.S. Fouda, H. Ibrahim, S. Rashwaan, A. El-Hossiany and R.M. Ahmed, Expired Drug (pantoprazole sodium) as a Corrosion Inhibitor for High Carbon Steel in Hydrochloric Acid Solution, *Int. J. Electrochem. Sci*., 2018, **13**, no. 7, 6327–6346. doi: 10.20964/2018.07.33

38. A. Habibiyan, B. Ramezanzadeh, M. Mahdavian and M. Kasaeian, Facile size and chemistry-controlled synthesis of mussel-inspired bio-polymers based on Polydopamine Nanospheres: Application as eco-friendly corrosion inhibitors for mild steel against aqueous acidic solution, *J. Mol. Liq*., 2020, **298**, 111974. doi: 10.1016/j.molliq.2019.111974
39. A.S. Fouda, M.A.A. El-Ghaffar, M. Sherif, A.T. El-Habab and A. El-Hossiany, Novel Anionic 4-Tert-Octyl Phenol Ethoxylate Phosphate Surfactant as Corrosion Inhibitor for C-Steel in Acidic Media, *Prot. Met. Phys. Chem. Surfaces*, 2020, **56,** 189–201. doi: 10.1134/S2070205120010086
40. Y. Baymou, H. Bidi, M.E. Touhami, M. Allam, M. Rkayae and R.A. Belakhmima, Corrosion Protection for Cast Iron in Sulfamic Acid Solutions and Studies of the Cooperative Effect between Cationic Surfactant and Acid Counterions, *J. Bio- Tribo-Corros*., 2018, **4**, 11. doi: 10.1007/s40735-018-0127-2
41. A.S. Fouda, E. Abdel-Latif, H.M. Helal and A. El-Hossiany, Synthesis and characterization of some novel thiazole derivatives and their applications as corrosion inhibitors for zinc in 1 M hydrochloric acid solution, *Russ. J. Electrochem*., 2021, **57**, 159–171. doi: 10.1134/S1023193521020105

♦ ♦ ♦